



More Electric Aircraft Forum

Power Quality and Stability Issues in More-Electric Aircraft Electrical Power Systems

Xinyun Liu, Andrew Forsyth
University of Manchester, UK

Hubert Piquet, Sylvain Girinon, Xavier Roboam, Nicolas Roux
Université de Toulouse, Laboratoire PLAsma et Conversion d'Énergie (LAPLACE), France

Antonio Griffo, Jiabin Wang
University of Sheffield, UK

Serhiy Bozhko, Pat Wheeler
University of Nottingham, UK

Matthieu Margail, Jerome Mavier, Lucien Prisse
Airbus France, France

Copyright © 2009 MOET Project Consortium – ALL RIGHTS RESERVED

ABSTRACT

This paper summarizes the work undertaken by four universities on various aspects of the power quality and stability in more-electric aircraft electrical systems. Research to identify the stability limits of multiple load systems, the design and optimization of HVDC filters, the impact of regeneration into AC buses, and active damping of HVDC distribution systems are described together with simulation results.

INTRODUCTION

The adoption of more-electric aircraft technologies offers the possibility of making weight and energy savings and reducing maintenance costs. However these technologies also create new challenges at the system level; predicting and preventing instability due to the “constant power” characteristics of motor drive equipment, handling the power that is regenerated by more-electric actuator equipment, and identifying globally optimal designs, for example to maximize the weight savings at a system level. This paper summarizes some of the research that has been undertaken in the MOET project to examine these issues.

The MOET Project Steering Committee has approved this paper for publication. The author is solely responsible for the content of the paper.



The MOET project, coordinated by Airbus France, is co-funded by the European Commission within the Sixth Framework Programme

<http://www.moetproject.eu>



An analysis method based upon symbolic computation has been developed at the University of Toulouse to assess the stability limits of multiple motor drives operating from a common DC bus. An optimization method for the design of the input filters in multiple motor drives has been developed at Sheffield University, showing the weight savings that may be achieved by optimizing the design at a system level. An alternative way to reduce the weight of the input filter in motor drives has been examined at the University of Manchester, showing that the passive damping branch in the filter may be reduced or eliminated using active damping techniques embedded in the motor drive controller. Lastly work at Nottingham University has shown the effect that transient regeneration of energy from actuator loads may have on the voltage quality of an AC power bus.

Due to the limited length of the paper, the contents are only a brief summary of each partner's work.

STABILITY LIMITS IN MULTI-LOAD SYSTEMS

This section concerns the possible interaction between equipment connected on an HVDC bus. These interactions can lead to unstable situations, which affect the operation both of the equipment and of the network, drastically reducing the quality of the electrical power distributed. In order to avoid these phenomena, the LAPLACE Lab has developed models, tools and a methodology to predict and control, by means of an adequate design, the stability of the whole system.

MODELLING OF THE EQUIPMENT

In the approach presented here, we focus on motor control unit (MCU) equipment, the structure of which is shown in Figure 1. A DC filter is inserted at the input of the inverter; various filter topologies are possible, which have the purpose of maintaining the quality

of both the absorbed current I_{IN} and the inverter voltage V_{DC} .

The whole drive system (inverter + PMSM + controller) is modelled, around a DC operating point (small variations model) by means of its equivalent admittance, which is analytically computed [1], with symbolic computation software (Maple [3]). The coefficients of the admittance are analytically developed, and they are functions of the physical parameters of the drive (inverter, PMSM, control loops).

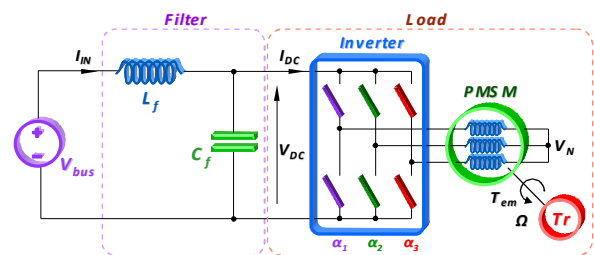


Figure 1 : MCU equipment

On this basis, various analyses of the drive associated with its input filter and implemented in an HVDC network can be achieved: a circuit analysis of the topology is realized and the transfer function, $T(s)$, relating the variations of the input voltage (V_{DC}) to the variations of the HVDC bus voltage (V_{bus}) is computed; this transfer function remains a symbolic expression, in which all the system parameters appear. These expressions may be used to size some parameters of the drive (the control loop for instance) as well as its input filter [1].

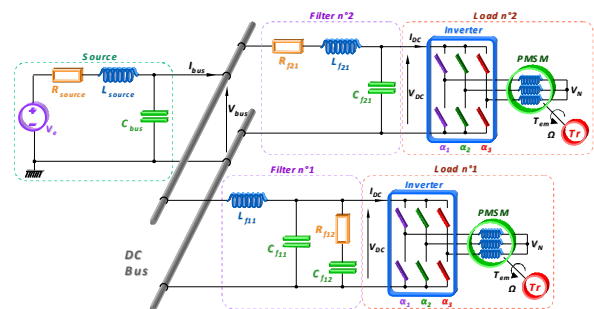


Figure 2 : HVDC network including two MCUs connected on the same DC bus

A library of input admittance models of various converters and loads has been developed; allowing an easy analysis of

different configurations. As can be seen in Figure 2, several MCUs (with different filter topologies) can be taken into account.

STABILITY ANALYSIS

The analytical expression of $T(s)$, although sometimes very complicated, contains all the information describing the dynamics of the whole system (network + connected loads). Its denominator $D(s)$, provides information about the stability. Using the Routh-Hürwitz criterion a set of *necessary and sufficient conditions*, analytical expressions may be obtained to analyze the stability of the HVDC network when some system parameters are varied.

For example Figure 3 shows the stability limits of two well-designed MCUs operating from a common DC bus through separate feeder cables, which tend to increase the filter inductances. The powers of the two loads are plotted against each other.

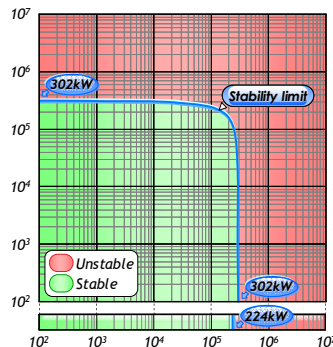


Figure 3 : HVDC network stability, according to the delivered powers (P_{Mcu1} vs P_{Mcu2})

The power limit, for only one drive is also presented and is seen to be smaller than in the first case with two loads. This example shows that it is preferable to spread the power delivery, between several loads, the worst case being a single very high power load.

DESIGN OPTIMIZATION OF HVDC FILTERS

This section describes research undertaken at the University of Sheffield on the optimization of DC filter components.

The supply and load filters have a significant influence on stability of an HVDC power system with power electronics controlled loads, such as MCUs, DC/DC and DC/AC converters. Although network stability is a fundamental prerequisite to proper functioning of the electrical power system, additional constraints should be taken into account in order to comply with power quality and transient behaviour requirements. Stability and power quality requirements impose constraints on the filter design which may be traded against each other optimizing a carefully chosen cost function. This could be the combined size and/or weight of the filter's components. Although significant savings can potentially be achieved with global optimization, fruitful discussions with Airbus-France electrical engineers suggested that, from an airframer's perspective, the design of an HVDC power supply and load filters should ideally be tackled by subdividing the global design problem into individual sub-problems, where the supply and each of the load filters are independently designed. This allows easier commissioning and integration of components from different suppliers. However this may not lead to a globally optimal solution.

By way of example, Figure 4 shows the schematic of an HVDC network with three loads, where Z_{eq} represents the equivalent impedance of the HVDC power source.

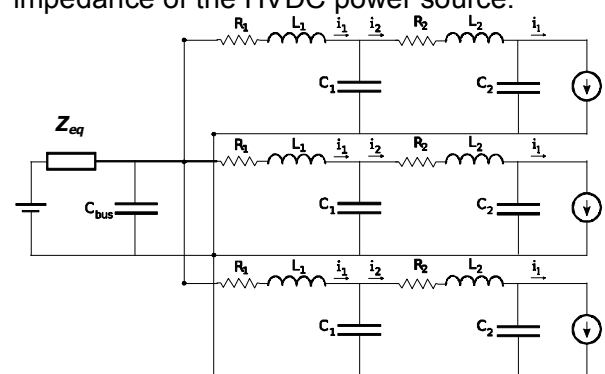


Figure 4. Schematic of an HVDC network

Based on recommendations from Airbus-France electrical network engineers [4], the filter design may be performed in three steps:

- (1) Determine the bus filter capacitance, C_{bus} , according to the impedance of the

HVDC source, and power quality and stability specifications assuming a constant power load equal to the total power of the system.

- (2) Determine filter parameters and control bandwidths of each filter-load subsystem according to power quality and stability specifications, assuming an ideal voltage source.
- (3) Compute the eigenvalues of the interconnected system to validate its global stability properties.

Step 2 should be performed via an optimization procedure, which, for minimum weight, can be formulated as:

$$\min_{x \in D} \{W(x)\}, \text{ subject to: } \begin{cases} f(x) \leq 0 \\ g(x) = 0 \end{cases}$$

where x denotes the parameter vectors. The inequality and equality constraints can be specified as stability (e.g. a minimum damping factor ζ) and power quality constraints (e.g. an assigned corner frequency). Weight variations of passive components can be established from manufacturer's datasheets [5][6] or via design analysis [7]. The power electronics controlled load may be treated as a constant power load (CPL), or its dynamic behaviour can be taken into account in the optimization process.

The influence of filter topologies on weight can also be investigated. The proposed optimization procedure has been applied to the 2nd, 3rd and 4th order filters. Each filter is individually optimized with respect to its weight, while imposing stability (damping factor $\zeta \geq 0.03$) and power quality constraints (same harmonic current attenuation of 10kHz switching frequency). The frequency responses of the weight-optimized 4th, 3rd and 2nd order filters are shown in Figure 5 for a 150kW constant power load. As can be seen, all designs achieve the same current harmonic attenuation (~ -55 dB) at 10kHz.

The use of the 4th order filter leads to a significant weight reduction by virtue of the increase in its corner frequencies. However,

it has less attenuation on frequencies below 10kHz. The minimised weights for the three filter topologies are compared in Table 1.

Table 1. Weight comparison of three filter topologies

	2 nd	3 rd	4 th
Total weight (kg)	25	19.3	14

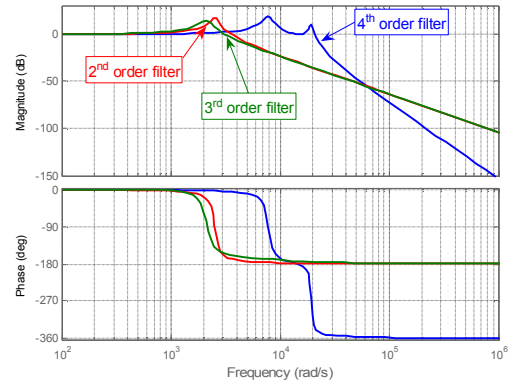


Figure 5. Frequency response of weight optimized 4th, 3rd and 2nd order filters for a 150kW load

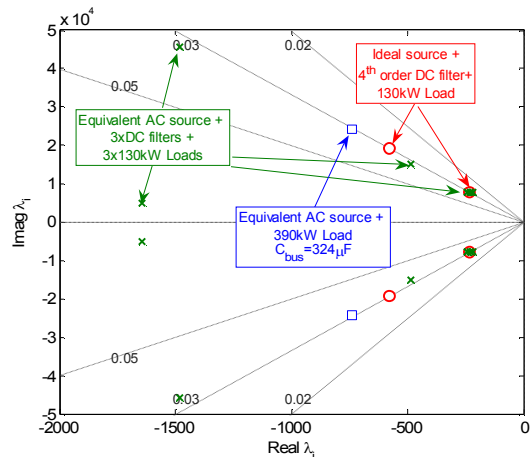


Figure 6. Distribution of eigenvalues

It is necessary to verify the stability of the interconnected system when each load filter, which is designed assuming an ideal voltage source is connected to a non-ideal common source, as shown in Figure 4. Without loss of generality, three 130kW constant power loads with their individually optimized 4th order filters are assumed. Figure 6 shows the eigenvalue distribution of the interconnected three load system with $C_{bus} = 324 \mu F$, which is sized against the total constant power of 390kW for $\zeta = 0.03$, together with the eigenvalue distribution of the system, which

consists of the source and the 390kW constant power load only, and the eigenvalue distributions of each filter-load sub-system. Again, it is evident that all eigenvalues of the interconnected source-multiple load system have their damping ratio greater than 0.03, which implies that the interconnected system maintains the desired stability properties of its separately designed subsystems.

A global optimization procedure is also applicable to the filter design of interconnected source-multiple load systems. By way of example, the global optimization procedure is applied to an interconnected system consisting of the same HVDC source which supplies two constant power loads of 130kW and 150kW via their 4th order filters. A total of 13 parameters are varied in the global optimization. The global optimization yields 11% weight reduction compared with the individually optimized design.

IMPACT OF REGENERATION INTO AC POWER BUS

This section describes work undertaken at Nottingham University to assess the impact of transient regeneration on the voltage quality of the AC bus.

POWER SYSTEM ARCHITECTURE STUDIED

The power system for the MOET Large Aircraft [8] is used as the basis for this study. Details of its operation under both normal and abnormal conditions can be found in [8]. For the purposes of a regeneration study one can exploit the important property of this architecture, namely that at no time can any of the power system buses be supplied by more than one source of electrical energy. Hence, the study is conducted using the generalized power system layout shown in Figure 7.

REGENERATION SCENARIO FOR THE STUDY

The main sources of regenerative energy in the onboard power system are the aircraft

actuation systems: ailerons, rudder, flaps, spoilers, horizontal stabilizers (HS) and others. Regeneration can occur either when an actuation system is requested to process a reference motion with aiding aerodynamic forces or when a fast response from an actuator is requested resulting in a high rate of deceleration. In the first case the source of regenerative energy is an aerodynamic force that acts on the flight surface in the same direction as the actuator movement. In the second case the regenerative energy comes from energy stored in the inertia of the moving actuator's parts.

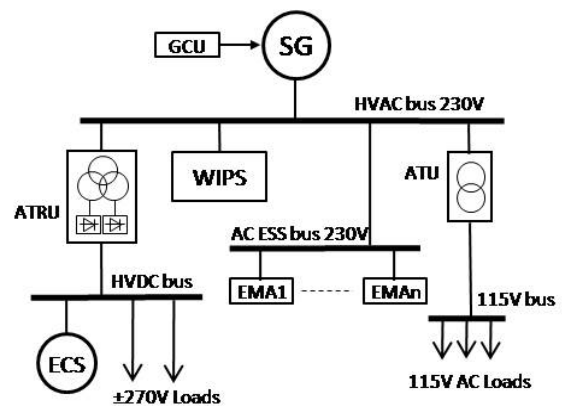


Figure 7. Generalized AC power system architecture

Assessment of possible regeneration regimes resulted in the identification of "normal" and "worst-case" scenarios for further simulation study. In all cases, the main contributions to the regenerative energy are the ailerons and rudder. The horizontal stabilizer is usually equipped with gears having a "no-back" facility that eliminates possible regeneration. The flaps and spoilers have a low dynamical response and their contribution to possible regeneration is negligible and is ignored in this study. Under normal conditions the rudder can produce up to 15kW of regenerative power for 100ms. The amount of regenerative power from the ailerons is evaluated as 165W for 100ms. Such regenerative events can occur every 10-12 seconds. Taking into account some safety margin, the "normal" regeneration scenario is assumed as a 100ms pulse of

17kW mechanical power on the actuator shaft.

Compared to the power system rating (225kW generator) the "normal" pulse of regenerative power is relatively small therefore one can expect the voltage on the buses to be maintained well within defined limits. Therefore, the power system was also studied under the condition of substantial regenerative power, which is unrealistic for normal flight conditions, but allows one to judge the system voltage control performance. Such a scenario assumes all the actuation systems simultaneously turn into a constant regeneration mode corresponding to their rated powers. For the MOET Large Aircraft [8] power system, this is equivalent to 55kW of regenerative power (on the mechanical side).

For both normal and worst-case scenarios the voltage transients are assessed against well-recognized standards [9] stipulating the envelope for aircraft voltage during normal transients.

SIMULATION RESULTS

Simulation of both scenarios has been undertaken in SABER. Results for the "normal" regeneration scenario are shown in Figure 8. The voltage of the HVAC bus remains well within the envelopes specified by MIL-STD-704F [9] (the "forbidden" zones are shown in red) during transients initiated by both rising and falling regenerative power pulse edges.

Simulation results for the worst-case scenario are depicted in Figure 9. Even for such a severe disturbance, the HVAC bus voltage (the bottom curve) remains within the envelope specified for the normal transients (shown by red dashed lines). This figure also shows the generator power and torque reducing due to the regenerative energy when the total actuator power (the top curve) goes negative.

Both normal and worst-case scenario simulations confirm that the HVAC bus

voltage complies with existing regulations. It should be noted that the GCU control for these simulations has not been validated against a real generator, however a common design methodology has been used.

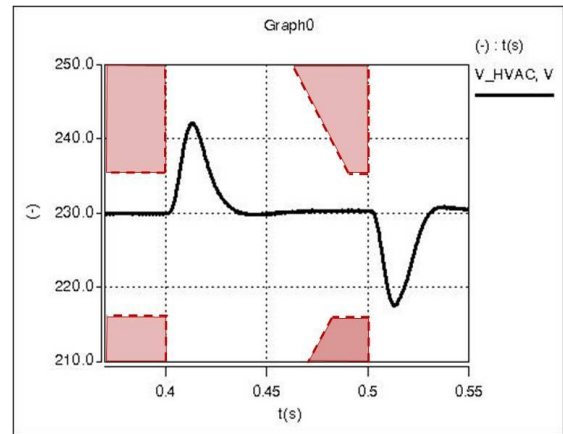


Figure 8. Simulation of normal regeneration mode

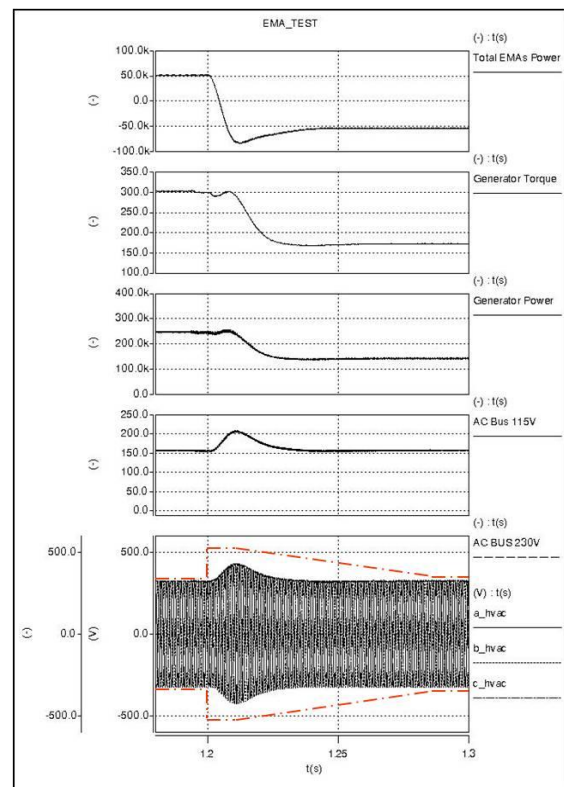


Figure 9. Simulation of worst-case regeneration mode

ACTIVE DAMPING OF HVDC DISTRIBUTION SYSTEM

ACTIVE DAMPING METHOD

This section describes work undertaken at Manchester University to reduce the size of HVDC filter equipment by using active damping techniques.

The passive damping branch that forms part of the high frequency input filter typically comprises a large DC-blocking capacitor and a resistor, C_d and R_d in Figure 10. These elements may be reduced or eliminated by programming the load equipment to provide the damping actively.

In this research, permanent magnet synchronous motor (PMSM) drive systems are used as loads connected to the 540V DC bus. The diagram of the drive system is shown in Figure 10 and the motor is modelled in the rotating d-q domain using the magnitude invariant version of the Park Transform [10].

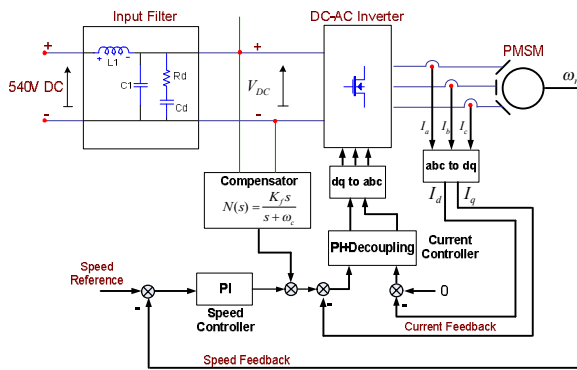


Figure 10. Diagram of the PMSM Drive System

An active stabilizing method is used in the MCU [11][12], which monitors the DC link voltage variation and stabilizes the drive system by injecting a small proportion of the DC link voltage variation into the current control loop as shown in Figure 10.

Small-signal analysis and averaged-value modelling techniques were used to derive the input admittance and characteristic transfer functions of the drive system with and

without the active stabilizing controller. It has been found that the active stabilizing controller can stabilize the system when used alone or in combination with the passive damping network (R_d+C_d). When used in combination with the passive damping, the values of C_d may be reduced below those required without active damping. The combinations of controller gain K_f and passive damping capacitance C_d resulting in constant damping factors are plotted in the upper part of Figure 11 with the left y-axis showing the reduction in C_d with increased K_f and the right y-axis showing the increase in the output torque to input voltage sensitivity transfer function $\delta T_q / \delta V_{DC}$ magnitude caused by the active damping, which is independent of the damping factor. In the bottom part of Figure 11 the magnitude of the frequency response of the sensitivity transfer function is plotted for the passively damped system and the mixed damped system with $K_f=1$ showing the increase of sensitivity over low and high frequencies.

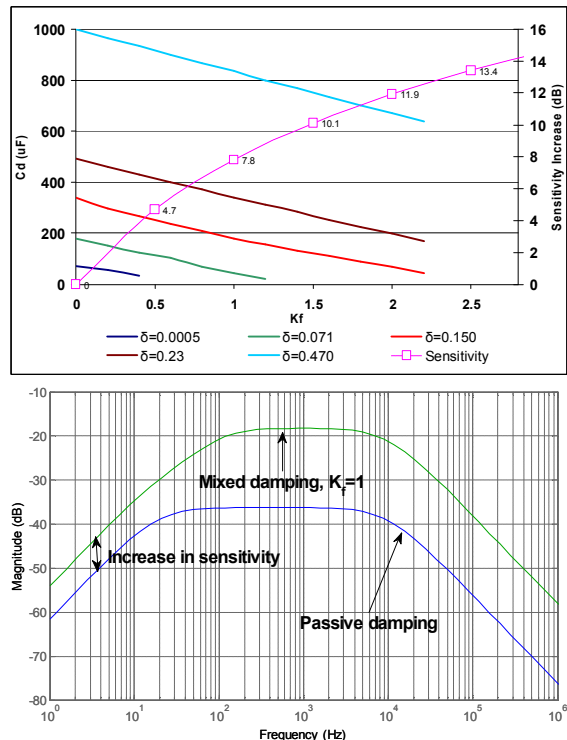


Figure 11. Reduction in C_d and increase in magnitude of sensitivity transfer function $\delta T_q / \delta V_{DC}$ for different K_f values

SIMULATION RESULTS

To demonstrate the use of the active damping technique, an HVDC distribution system with two loads as shown in Figure 12 was simulated in Saber with three different damping techniques, namely purely passive damping (only a passive damping network is used), purely active damping (only an active stabilizing controller is used) and mixed damping (both a passive damping network and an active stabilizing controller are used).

A source filter representing the output of a multi-phase rectifier is also included (R_{src} , L_{src} and C_{src} in Figure 12). To make a fair comparison, the parameters of the passive damping network and active stabilizing controller are designed so that the passively damped and mixed damped systems have the same damping factor 0.31 in the source and load filter poles. The actively damped system is designed to have the same source filter damping factor as the passively damped system and a heavier damped load filter ($\delta=0.51$) because the controller gain K_f is the only adjustable parameter. The resulting parameters are listed in Table 2. $L_1=20\mu\text{H}$, $L_2=20\mu\text{H}$, $C_1=360\mu\text{F}$, $C_2=220\mu\text{F}$, $L_{src}=100\mu\text{H}$, $C_{src}=1\text{mF}$, $R_{src}=0.1\ \Omega$, Load1 power=96kW, Load2 power=20kW

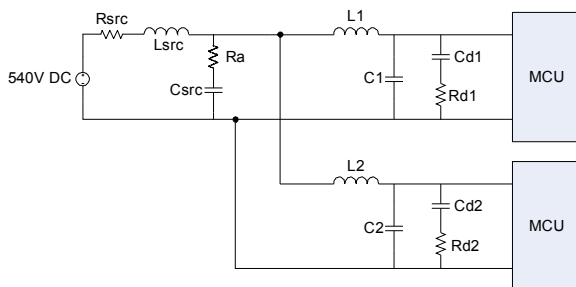


Figure 12. Two-load HVDC system

The simulation results are shown in Figure 13, where a step increase from 540V to 560V was applied to the DC supply. The purely active damped system responses are plotted in pink lines. The purely passive damped system responses are in yellow lines and the mixed damped system responses are in black. Figure 13 shows from top to bottom the two motor speeds, the DC link current,

DC link voltage, the input voltages to the load and the input filter inductor currents. It can be seen that the active stabilizing method can effectively stabilize the system and achieve a similar damping effect in the DC link voltage and current at a cost of an increased deviation in motor speed during the transient.

Table 2. Filters and stabilizing controller parameters

	$R_a(\Omega)$	$Cd_1(\mu\text{F})$	$Rd_1(\Omega)$	$Cd_2(\mu\text{F})$	$Rd_2(\Omega)$	K_f
Passive	0.15	285	0.44	142	0.46	0
Mixed	0	179	0.64	82	0.58	1
Active	0	0	∞	0	∞	1.3

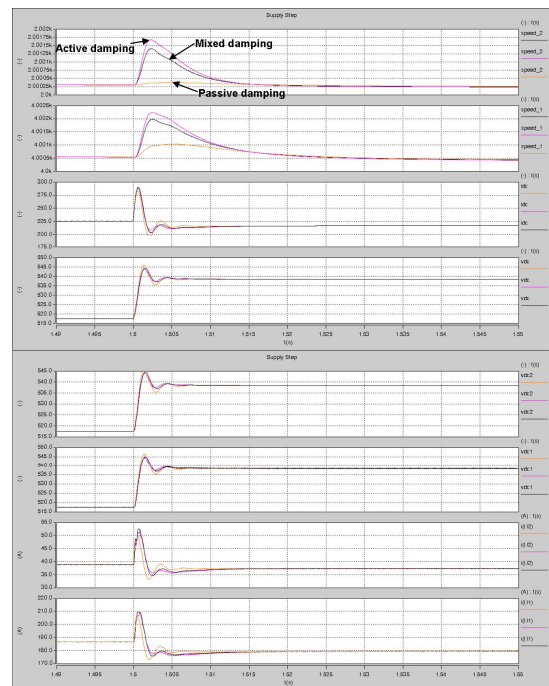


Figure 13. Response to a supply voltage step increase from 540V to 560V

CONCLUSION

A modelling and stability analysis method based on symbolic computation has been described that may be extended to incorporate a larger number of load elements. A design and optimization procedure has been described for the HVDC filters in a multiple load system, highlighting the potential weight savings of undertaking a system-level optimization. A simulation study on the MOET Large Aircraft architecture has shown that transient regeneration from

actuator loads does not adversely affect the system power quality. Finally the use of active damping has been shown to offer a viable way to reduce the requirement for large passive damping elements in HVDC filters. However, the use of active damping will result in increased MCU sensitivity to DC link voltage disturbances.

ACKNOWLEDGMENTS

The MOET project is a European Project, co-funded by the European Commission within the Sixth Framework Programme.

REFERENCES

1. "Analytical modeling of the input admittance of an electric drive for stability analysis purposes", S. Girinon, C. Baumann, H. Piquet, and N. Roux – European Physical Journal (EPJ)
2. "Input filter considerations in design and application of switching regulators", R. D. Middlebrook, Proc. IEEE Industry Applications Society Annual Meeting, pp. 366–382, 1976.
3. Maple®, <http://www.maplesoft.com>
4. Airbus-France memo, "MOET – 724 – A-F – MCM –Source & load specification – 1 – 08-R1.0", October 2008
5. Westcode Semiconductors Ltd, "Capacitors for power electronics"
6. Vishay, "Fixed wirewound high power resistors"
7. S. Chandrasekaran, S.A. Ragon, D.K. Lindner, Z. Gurdal, D. Boroyevich, "Optimization of an aircraft power distribution system", Journal of Aircraft, vol. 40, n.1, 2003, pp. 16-26
8. Electrical System Architecture V0. Specification and Description (D3.11.1). MOET-SWP3.11-AF-DEL-Elec_Syst_Arch_V0-001-06-0.1
9. MIL STD 704, "Revision F - Aircraft Electric Power Characteristics"
10. P. Pillay, and R. Krishnan, "Modeling, simulation, and analysis of permanent-magnet motor drives. I. The permanent-magnet synchronous motor drive," Industry Applications, IEEE Transactions on , 1989, vol.25, no.2, pp. 265 - 273
11. X. Liu, A.J. Forsyth and A.M. Cross, "Negative Input-Resistance Compensator for a Constant Power Load," IEEE Transactions on Industrial Electronics, 2007, vol.54, no.6, pp. 3188 – 3196
12. X. Liu, and A.J. Forsyth, "Active Stabilisation of a PMSM Drive System for Aerospace Applications", Proc. of IEEE Power Electronics Specialists Conference, PESC, 2008

CONTACT

Andrew Forsyth, School of Electrical and Electronic Engineering, University of Manchester, Manchester M60 1QD, UK.
Email: andrew.forsyth@manchester.ac.uk

Jiabing Wang, Department of Electronic and Electrical Engineering, University of Sheffield, UK.
Email: j.b.wang@sheffield.ac.uk

Pat Wheeler, School of Electrical and Electronic Engineering, The University of Nottingham, Nottingham NG7 2RD, UK.
Email: pat.wheeler@nottingham.ac.uk

Hubert Piquet, Université de Toulouse, Laboratoire PLASMA et Conversion d'Énergie (LAPLACE), CNRS (UMR 5213), INPT, UPS, 2 rue Camichel, BP 7122, 31071 Toulouse Cedex 7, France.
Email : Hubert.Piquet@laplace.univ-tlse.fr

Matthieu Margail, Prospective Group - EDYNE3, Airbus France, PO Box M3001, 31060 Toulouse Cedex 9, France
Email : Matthieu.MARGAIL@airbus.com

DEFINITIONS, ACRONYMS, ABBREVIATIONS

- **MEA** *More Electric Aircraft*
- **HVDC** *High Voltage Direct Current*
- **MCU** *Motor Control Unit*